Title
INITIAL STATES OF OXIDATION OF THE Pt3Ti(111) AID (100) SINGLE CRYSTAL SURFACES

Authors
Bardi, U.
Ross, P.N.

Publication Date
1984-05-01

Lawrence Berkeley Laboratory
UNIVERSITY OF CALIFORNIA

Materials & Molecular Research Division

Submitted to the Journal of Vacuum Science and Technology

INITIAL STATES OF OXIDATION OF THE $Pt_3Ti(111)$ AND (100) SINGLE CRYSTAL SURFACES

U. Bardi and P.N. Ross

May 1984

Prepared for the U.S. Department of Energy under Contract DE-AC03-76SF00098

DISCLAIMER

LBL-17869

INITIAL STAGES OF OXIDATION OF THE Pt_3Ti(111) and (100) SINGLE CRYSTAL SURFACES

U. Bardi† and P.N. Ross

Lawrence Berkeley Laboratory
University of California
Berkeley, California 94720

May 1984

†Present address: Dipartimento di Chimica, Universita de Firenze, 50121 Firenze, Italy.

ABSTRACT

The process of segregation of titanium oxides onto the surface of Pt_3Ti upon the exposure to oxygen at different pressures and temperatures was studied by LEED and AES. Oriented [111] and [100] monocrystals as well as polycrystals were synthesized for study. Qualitatively similar behavior was observed with all three types of surfaces, with three stages of oxidation observed on each surface. A layer of stoichiometry close to TiO segregated onto the surface in the initial stage of oxidation, depleting the subsurface region of the alloy in Ti. The TiO formed a compact, epitaxial monolayer which completely blocked the metallic surface for chemisorption by carbon monoxide. Further oxidation caused formation of a multilayer of $TiO_{1.2}$, an oxide with an orthorhombic structure derived from TiO by removing Ti atoms to form an ordered vacancy lattice. Finally oxidation at the relatively extreme conditions of atmosphere pressure at high (> 1000 K) temperature caused formation of thick TiO_2 (rutile) overlayers.

INTRODUCTION

Pt_3Ti is among the stablest of all intermetallic compounds. Its high heat of formation (-70.5 kcal/mole(1)) can be interpreted in terms of the Engel-Brewer model of the intermetallic bond (2). In this model the strength of the bond results from the interaction of d-shell electrons of both metals. The perturbation of the electronic states in both metals due to intermetallic bond formation might be expected to cause changes in the catalytic properties of Pt_3Ti in comparison to pure Pt. The catalytic interest of the Pt_3Ti compound led us to a detailed study of the adsorptive properties of the clean surface, which indicated (3) the presence of ligand effects in the absence of oxygen on the surface. However, thermodynamic considerations indicate that Pt_3Ti should oxidize with the formation of titanium oxide in the presence of oxygen. Therefore, a detailed study of the oxidation process appeared to be a fundamental step in the understanding of the mechanism of catalysis by Pt_3Ti and other Pt intermetallic compounds in oxidizing atmospheres (4).

We found that upon exposure to oxygen titanium segregates from the bulk of the alloy to the surface to form a layer of titanium oxide. The oxidation process is very slow at room temperature and practically non-existent at very low pressure. However oxidation takes place even at very low pressure at sufficiently high temperature. Using LEED we have been able to characterize the titanium oxide phases growing on the single crystal surfaces. Initially the oxide grows as a monolayer (2D) phase of probable TiO stoichiometry. Further oxidation leads to the formation of a multilayer which is formed (at least in some conditions) by three-dimensional phases growing on the surface which appeared to be structurally related to the

orthorhombic oxide $TiO_{1.20}$. Finally, at high temperature and atmospheric pressure, a thick film of TiO_2 (rutile) forms on the surface.

EXPERIMENTAL

Polycrystaline Pt_3Ti was prepared arc-melting the component metals in inert gas atmosphere (Ti nominal purity: 99.97%). The formation of the cubic form of the alloy (Cu_3 Au type) was checked by x-ray diffraction. Polycrystalline samples were spark cut in the shape of small disks and mechanically polished before introduction in the UHV system.

To obtain a single crystal, the polycrystalline material was zone refined in vacuum until recrystallization took place. The formation of a single crystal was evidenced by the Laue back-diffraction pattern. Single crystal samples oriented along the [111] and [100] axes were spark cut and polished as the polycrystalline ones.

All samples were gold brazed on a Ta plate suspended by Ta wires, used also for resistive annealing (up to about 1200 K). Experiments were performed in a conventional UHV chamber equipped with LEED optics, single pass CMA with grazing incidence electron gun for AES, quadrupole mass spectrometer and facilities for Ar^+ bombardment. Oxygen could be introduced in the chamber through a leak valve up to about 5×10^{-5} torr with simultaneous pumping.

RESULTS

3.1 LEED RESULTS

As described previously (3), the Pt_3Ti surface, either single crystal or polycrystalline, could be cleaned in UHV by a combination of ion bombardment, oxygen dosing and annealing. The LEED results for the clean Pt_3Ti (111) and (100) surfaces were reported recently (5) and, together with the

surface concentration determined by AES were shown to be consistent with surfaces resulting from the simple truncation of the bulk structure. The observed patterns have been indexed in (5) as superstructures of the fcc (111) and (100) unit cells. Such a notation is possible here since in the alloy and in the pure Pt unit cells the interatomic distances are the same within less than the 1% and the alloy structure can be obtained from the Pt structure by orderly substitution of part of the Pt atoms with titanium atoms. Using the "superstructure" notation, the LEED pattern observed on the $Pt_3Ti(111)$ surface has been described as a p(2x2) and the pattern on the $Pt_3Ti(100)$ as a c(2x2).

In the present paper we will continue using the superstructure type notation, and all the oxide superstructures will be indexed in relation to the (1x1) platinum unit cell. The use of this notation is essential here, since, as it will be described later, oxidation destroys the intermetallic (p(2x2) or c(2x2)) periodicity, leaving only the (1x1) platinum cell detectable by LEED.

3.1.1 $Pt_3Ti(111)$

Upon dosing the clean alloy surface with oxygen at 600 K and $1x10^{-7}$ torr, we detected traces of the pattern shown in Fig. 1a. This pattern is apparently due to oxidized titanium as indicated by the appearance of the oxygen AES peak and by the increase in the intensity of the titanium AES peaks. Traces of this pattern could be detected even at relatively low values of the Ti(387 eV)/Pt(237 eV) AES ratio, i.e. at a ratio of 1.9 compared to the value of 1.7 for the clean surface. The pattern intensified upon more extensive oxidation with higher values of the Ti/Pt AES ratio. The interpretation of this pattern is also shown in the figure,

taking into account that some of the spots are the result of double diffraction. In matrix notation, the pattern can be described as $\begin{bmatrix} 1.20 & \overline{0.14} \\ 0 & 1.24 \end{bmatrix}$. The unit cell is oblique (quasi-hexagonal) with the two base vectors respectively 3.4 and 3.5 Å long, forming an angle of 125.5°. Two domains rotated by 11° are present. The presence of double diffraction features indicates that this pattern is due to a two-dimensional (2D) structure on the surface. During the initial phases of formation of this phase, while the layer occupied only a fraction of the substrate surface, the p(2x2) substrate pattern was still detectable. However, upon completion of the layer (a Ti (387 eV)/Pt(237 eV) ratio approaching 3.4), the p(2x2) spots disappeared, leaving only the (1x1) platinum spots superimposed on the quasi-hexagonal pattern. This change in the periodicity of the substrate surface is most easily interpreted in terms of titanium depletion of the subsurface layer(s), although simple disordering might also explain it.

Upon oxidation at higher temperature of a surface showing the quasi-hexagonal pattern, and subsequent rapid cooling (≈20 deg/sec), we detected the pattern shown in Fig. 1b. This pattern is superimposed on the quasi-hexagonal pattern. Several equivalent unit cells can be chosen for this phase. A possible one is oblique, with the two base vectors forming an angle of 108°, describable in matrix notation as $\begin{bmatrix} 0.53 & \overline{1.96} \\ 1.43 & 1.43 \end{bmatrix}$ (see Table 1). We can also choose a centered rectangular cell, $\begin{bmatrix} 2.5 & \overline{2.5} \\ 1.43 & 1.43 \end{bmatrix}$ in matrix notation. The latter type of cell will be used preferentially here since the rectangular symmetry of the lattice is more evident. We note that three equivalent domains could form on the $Pt_3Ti(111)$ surface, but only one could be detected by LEED. The other two seem to be present, but very

weak. The absence of double diffraction features indicates that this pattern corresponds to the formation of more than one layer on the surface. This phase has been observed for Ti(387 eV)/Pt(237 eV) ratios from about 6.0 to higher than 12.0.

In the discussion section, we shall compare the lattice parameters of the $\begin{bmatrix} 2.5 & \overline{2.5} \\ 1.43 & 1.43 \end{bmatrix}$ structure with those of known titanium oxide bulk phases. On the basis of this comparison, this oxide has been identified as "$TiO_{1.20}$." Table 1 summarizes all the oxide phases observed on Pt_3Ti (111).

3.1.2 $Pt_3Ti(100)$

Upon exposure to oxygen, we observed on this face a larger number of patterns than on the (111) face. Three distinct patterns corresponding to single layer phases, as evidenced by the presence of double diffraction features, were observed. The formation of these patterns was dependent on temperature: the pattern obtained by exposure to oxygen at 773 K can be described as $\begin{bmatrix} 1.5 & 0 \\ 0 & 1.2 \end{bmatrix}$ in matrix notation (Fig. 2a); another pattern appeared for exposures at 800-1000 K, in matrix notation described as $\begin{bmatrix} 2.0 & \overline{0.3} \\ 0 & 1.2 \end{bmatrix}$ (Fig. 2b); the third pattern has hexagonal symmetry $\begin{bmatrix} 1 & \overline{0.57} \\ 0 & 1.14 \end{bmatrix}$ and formed upon exposure to oxygen at temperatures higher than about 1000 K at low ($<10^{-6}$ torr) oxygen pressure (Fig. 2c). This pattern formed also by annealing at high temperature one of the other 2D phases. The AES data indicate that the hexagonal structure was characterized by a lower oxygen content, that is, the lowest O/Ti ratio was observed for the hexagonal phase. Similarly to the behavior observed on the Pt_3Ti (111) surface, on the (100) the c(2x2) intermetallic periodicity was still detectable in the initial phases of formation of the overlayer phases (see Fig. 2a). However, the c(2x2) type spots weakened and disappeared upon completion of a monolayer

of oxide ("TiO") indicating a probable depletion in titanium in the subsurface layers.

Upon oxidation at T > 1000 K and $P_{O_2} = 10^{-7}$ torr, we observed the formation of a Ti(387 eV)/Pt(237 eV) AES ratio greater than 5.0 and the LEED pattern shown in Fig. 3d. This pattern has parameters which are similar to those of the $\begin{bmatrix} 2.5 & \overline{2.5} \\ 1.43 & 1.43 \end{bmatrix}$ pattern observed on the (111) face. As in that case we can choose a primitive (oblique) unit cell $\begin{bmatrix} 1.0 & \overline{2.1} \\ 1.0 & 0.9 \end{bmatrix}$, or a centered rectangular unit cell $\begin{bmatrix} 3.0 & \overline{3.33} \\ 1.0 & 0.9 \end{bmatrix}$. As on the (111) face, the rectangular representation of the overlayer will be used preferentially. In the LEED pattern in Fig. 2d two equivalent domains rotated of 5.7° with respect to each other are apparent. Also double diffraction spots are detectable, indicating that this phase formed from uniform 2D overlayers; double diffraction spots were not observed from the multilayer phase on the (111) face. Another difference from the (111) face was that here the formation of the $\begin{bmatrix} 3.0 & \overline{3.33} \\ 1.0 & 0.9 \end{bmatrix}$ phase resulted in the disappearance of any other 2D phase previously present on the surface. However the double diffraction features disappeared in concomitance with a general weakening of the pattern by annealing the surface in vacuum over about 1000 K. The annealing also had the effect of causing the formation of the $\begin{bmatrix} 2.0 & \overline{0.3} \\ 0 & 1.2 \end{bmatrix}$ pattern superimposed on the $\begin{bmatrix} 3.0 & \overline{3.33} \\ 1.0 & 0.9 \end{bmatrix}$ pattern. If the annealing was protracted for several minutes the $\begin{bmatrix} 1 & \overline{0.57} \\ 0 & 1.14 \end{bmatrix}$ pattern could also be detected. Complete disappearance of the $\begin{bmatrix} 3.0 & \overline{3.33} \\ 1.0 & 0.9 \end{bmatrix}$ pattern could be obtained by a long annealing at these temperatures. These LEED observations coupled with the AES data (described in Sec. 3.2) indicate that upon vacuum annealing a decomposition of the oxide overlayer takes place accompanied by dissolution of Ti back into the substrate. This dissolution process will be discussed at length in another

section. As in the (111) surface case, the multilayer phase has been identified as "$TiO_{1.20}$." The titanium oxide phases observed on the Pt_3Ti (100) surface are summarized in Table 2.

3.2 Surface Composition Analyses by AES

The only mechanism of oxygen uptake observed on Pt_3Ti was the formation of titanium oxide, as evidenced by the simultaneous growth of the intensity of both the Ti and O AES peaks. Oxygen chemisorption (i.e. TDS desorbable oxygen) was not observed. In what follows we will use the ratio of the two most intense Ti and Pt AES transitions (respectively at 387 and 237 eV) as a measure of the amount of oxide on the surface. As it will be described in detail later, the AES ratio of the oxygen and platinum AES peaks was not suitable for such a measure, since the degree of oxidation of the surface titanium oxide phases could vary as a function of the conditions of exposure.

3.2.1 Stoichiometry of Overlayers

In general, we did not observe by AES any significant different in the oxidation behavior of the three types of surfaces studied (single crystal (100) and (111) and polycrystalline). This observation is illustrated by the AES data in Fig. 3. The dispersion of points observed is mainly due to factors such as small variations in the residual surface carbon (contamination) and to variations in the residual pressure of reducing gases (H_2 and CO) in the vacuum chamber. As a consequence, in the rest of this section we have not categorized our results according to the structure of the surface, except when describing specific experiments.

The stoichiometry of the overlayer was observed to be very sensitive to the oxygen dosing conditions, as shown by the variations in AES peak

ratios with temperature and O_2 pressure in Figures 3 and 4. Essentially two stoichiometries were observed, which, as we shall describe in subsequent discussions, were identified as "TiO" and "$TiO_{1.2}$." The stoichometry which formed depended on both the temperature and pressure of dosing. At the selected temperature of 773 K, the curves in Fig. 3 clearly illustrate the formation of two different stoichiometries as a function of O_2 pressure. The first was produced by dosing at $< 10^{-6}$ torr O_2, which initiated the growth of the 2D (submonolayer) phase we identify as "TiO"; the complete monolayer) 2D phase was characterized by a Ti(387 eV)/Pt(237 eV) AES ratio of ca. 3 and a (508 eV)/Ti(387 eV) AEs ratio of ca. 0.8. Higher pressure dosing, at $5x10^{-6}$ torr O_2, increased the oxidation state of the Ti in the overlayer (from the increase in the O/Ti AES ratio to ca. 1.5) and increased the overlayer thickness (from the increase in the Ti/Pt AES ratio to ca. 5). This second stage of growth initiated the multilayer development of the phase we identify as "$TiO_{1.2}$"; progressive thickening of the "$TiO_{1.2}$" was observed when the dosing pressure was increased to $5x10^{-5}$ torr O_2. It is clear that this thickening occurred at constant stoichiometry, since the dramatic increase in the Ti/Pt AES ratio was accompanied by essentially no change in the O/Ti AES ratio. The variable temperature curves in Fig. 4 also illustrate a conversion in overlayer stoichiometry with increasing dosing temperature at a constant, relatively low dosing pressure of $1x10^{-6}$ torr O_2. At low temperature the 2D (submonolayer) phase is close to the "$TiO_{1.2}$" multilayer phase stoichiometry, but increasing temperature resulted

in the growth of a second layer (from the increase in Ti/Pt ratio from 2 to 4) of nominal stoichiometry "TiO" rather than "$TiO_{1.2}$." However, at this relatively low O_2 pressure, progressive thickening of multilayers of the "TiO" structure was not observed even at elevated (> 1000 K) temperature. We always observed that the multilayer structures were characterized by O/Ti AES ratios of ca. 1.5, identified as "$TiO_{1.2}$," and the 2D structures (or nearly 2D structures) were characterized by O/Ti AES ratios of 0.7-1.2. Table 3 summarizes the AES results and the general dosing condition which produced the characteristic stoichiometries. The "$TiO_{1.2}$" multilayers were relatively resistant to oxidation to "TiO_2" even at very high (several torr) pressure, provided the temperature was below ca. 1000 K. Nonetheless, atmospheric oxidation above 1000 K converted "$TiO_{1.2}$" multilayers to "TiO_2" and, depending on the time of exposure caused the growth of very thick (several micron) "TiO_2" overlayers, identified as the rutile structure by x-ray diffraction, characterized by an O/Ti AES ratio of 2.8.

3.2.2 Determination of Oxide Coverage

A combination of AES observations and chemical titration by CO can be used to determine the presence of metallic sites on the alloy surface and therefore measure the coverage of the (inert) titanium oxide segregated on the surface as a function of the Ti/Pt AES ratio. The CO molecule is a useful titrating agent since, as reported previously (3), it is adsorbed undissociated on the clean Pt_3Ti surface, and the titanium oxide covered surface does not adsorb CO. The CO TDS spectra from the partially oxide covered Pt_3Ti surface were complicated by the concomitant formation of CO_2 by reaction of the oxide directly with CO, but the CO_2 evolution occurred at a higher temperature than the peak in the CO TDS spectrum (at 390 K) and

a relatively small fraction of the CO adsorbed reacted with the oxide to form CO_2. From the plot of the intensity of the CO TDS peak at 390 K as a function of the Ti(387 eV)/Pt(237 eV) AES ratio (Fig. 5), we could determine that total blocking of all CO adsorption occurred at a ratio higher than about 3.4. The blocking coverage determined by the TDS measurements were also confirmed by AES data. Undissociated CO can be detected by AES by the characteristic double carbon peak (7), and this double peak could not be observed - indicating no CO adsorption - for a Ti(387 eV)/Pt(237 eV) higher than 3.5. From the experimental value of the Ti/Pt AES ratio corresponding to the total blocking of the surface, we could confirm the LEED results indicating the formation of a uniform 2D titanium oxide phase on the surface. An estimate of the expected Ti(387 eV)/Pt(237 eV) AES ratio, taking "reasonable" values for the electron mean free path (from 4 to 9 Å (7)) and assuming a compact titanium layer with the structure of the TiO (111) plane, gives a value which is an agreement with the observed ratio. These observations collectively reasonably preclude the possibility that the oxide grows from the start by the formation of multilayer (3 or 4 layers) "clusters" coexisting with bare metallic surface.

3.2.3 Determination of the Ti Valence State

The AES spectrum of titanium is a complex envelope of peaks in the region from 350 to 450 eV. These peaks involve transitions from the valence band and their shape has been shown to be sensitive to variations in the chemical environment (8). In (5) we reported that the ratio of the two main Ti peaks (387 and 416 eV) in the Pt_3Ti alloy is similar to that of the oxide and very different from that of titanium metal. As reported by Davis, et al. (8), fine features in the Ti AES spectrum permit the

distinction among the different degrees of oxidation of the titanium oxide: the higher oxides (Ti_2O_3 and TiO_2) are characterized by the presence of a small peak at about 395 eV which is absent in the oxide TiO and in Ti metal. As shown in Fig. 6, in the AES spectrum of titanium oxide segregating on Pt_3Ti, the 395 eV peak is absent in the formation of 2D phases, but this peak did appear upon the formation of a multilayer. This result indicates that the stoichiometry of the single layer phases is probably "TiO," while the multilayer has a higher oxygen content, an observation also confirmed by the values of the observed O/Ti AES ratios indicated in Table 3.

3.2.4 Kinetics of Oxide Overlayer Reduction

As indicated by the thermochemical data for Pt_3Ti (1), titanium oxide overlayers will be reduced and Ti dissolved into the substrate in the presence either of a reducing agent, or by thermal annealing at very low oxygen partial pressures. In Fig. 7 we show the results relative to the reduction of the oxide overlayer upon exposure to H_2 at increasing temperatures. The initial titanium oxide coverage was approximately two layers of "$TiO_{1.2}$." The hydrogen pressure reported was the highest pressure that could be maintained in the vacuum chamber in flow conditions. Two different processes occur in Fig. 7. In the first phase of reduction (T=300-573 K), the oxygen signal becomes considerably smaller, both with respect to the Pt and Ti signals. The Ti/Pt ratio, on the contrary, increases. Here the variation of the oxygen signal indicates a partial reduction of the oxide layer to reach a more stable stoichiometry. The increase of the Ti signal may derive from a partial reconstitution from the bulk in the titanium content of the subsurface layers, depleted in titanium upon oxidation. Actual decomposition of the titanium oxide layer and realloying

occurs only over 873 K. The reduction of the Ti/Pt AES ratio indicates the dissolution of titanium into the bulk, while oxygen is desorbed as H_2O. The O/Ti AES ratio remained approximately constant, indicating that dissolution of Ti occurred at constant O/Ti stoichiometry (which was slightly lower than that for "TiO").

A similar reduction in the O/Ti AES ratio to that shown in Fig. 7 was observed in the absence of intentional dosing with reducing gases, that is simply annealing in vacuum, but significantly higher temperatures (> 1000°K) were required. This process may involve actual O_2 desorption - not detected by mass spectrometry because of the weakness of the signal - or it may result either from oxygen dissolution into the Pt_3Ti bulk or by reaction with background gases in the UHV system.

DISCUSSION

According to the Engel-Brewer model of the intermetallic bond (2), the alloys of metals of the VIIIB group with metals of the IVB group are especially stable. This stability derives from the interaction of electrons in the d shell of both metals. In the case of Pt_3Ti, according to Brewer, the partially filled d-orbitals of Pt (d^7sp^2) mix with the unfilled d-orbitals of Ti (d sp) with the result of producing very strong intermetallic bonds. The thermodynamic properties of Pt_3Ti have been studied by Meschter and Worrell (1) who reported a highly negative heat of formation (-70.5 kcal/mole). One consequence of the high stability of the Pt-Ti bond is that, at sufficiently low oxygen pressures, titanium oxides can be reduced by reaction with Pt metal. However, titanium is a highly electropositive metal, and despite the strong bond with Pt, will tend to separate

from the alloy to form oxides in the presence of oxygen. This conclusion derives from simple thermodynamic calculations which show that at any measurable oxygen pressure (and in the absence of reducing agents), in the reaction:

$$Pt_3Ti + O_2 \rightleftharpoons TiO_2 + 3\ Pt$$

equilibrium is shifted to the right. For instance, at 1300 K the equilibrium oxygen pressure is as low as 10^{-12} torr; Pt_3Ti must therefore be considered metastable in air. However, no extensive (i.e. bulk) phase separation takes place in air at room temperature since the surface forms passivating thin films. Platinum does not form an oxide in air at low temperature (9) so that the passivation mechanism involves, as expected, the formation of a surface layer of a titanium oxide, much in the same way as titanium metal passivates. In agreement with the thermodynamic predictions, we found that surface oxidation of the Pt_3Ti alloy could be obtained at oxygen pressures as low as 10^{-7} torr, but only at high temperature. The initial resistance to oxidation at room temperature can be explained by kinetic factors, i.e. oxidation is an activated process due to the energy necessary to transfer Ti atoms from below the surface <u>onto</u> the surface in order to form the oxide. At moderate temperatures ($< 1000^{\circ}$ K), the oxidation process does cause surface segregation of Ti and formation of TiO- like overlayers whose thickness depends on O_2 pressure. A similar resistance to oxidation was found in the case of the Pt/Zr system (10).

We also found that the reverse reaction, i.e. the decomposition of the oxide overlayer and dissolution of Ti, could be obtained by annealing either in the presence of reducing agents (H_2, or CO) or simply annealing

in vacuum. In the latter case, however, the reaction slowed at an early stage beyond which little further reduction could be observed. It appears likely that in this case the mechanism of oxygen removal was dissolution into the Pt_3Ti bulk. This would lead to a rapid saturation with consequent blocking of further dissolution. On the other hand, in the presence of a reducing agent, the product of the oxide decomposition (H_2O, CO_2) was gaseous and therefore oxygen was removed immediately from the surface region permitting a further progress of the reaction.

Our observations indicate that the first step in the oxidation process of Pt_3Ti involves the formation of a uniform 2D titanium oxide phase on the surface. This is deduced mainly from the presence of double diffraction features in the LEED patterns. Double diffraction occurs when a diffracted beam coming from the substrate is diffracted a second time passing through the overlayer. It can only be observed when the overlayer is thin (otherwise the doubly diffracted beam would be attenuated by the passage through the overlayer) and covers a large fraction of the surface (otherwise the effect of the presence of the overlayer would be weak). Changes in the Ti/Pt AES peak ratios upon oxidation were also consistent with uniform 2D layer model. From the shape of the titanium AES peaks we could also determine that the stoichiometry of the initial 2D phase is "TiO." This conclusion was supported by considerations on the unit cell dimensions derived from LEED data. Consider for instance the $\begin{bmatrix} 1.20 & \overline{0.14} \\ 0 & 1.24 \end{bmatrix}$ phase observed on Pt_3Ti (111). If we assume that the titanium atoms form a quasi-hexagonal plane (in analogy with the TiO (111) plane) bonded to the substrate and that the oxygen atoms are situated on top of the titanium

layer, then the unit cell dimensions (3.4 by 3.5 Å, α = 125.5°) are too small to fit more than one atom (Ti or O) per cell in the same plane. Therefore, the O/Ti atomic ratio must be 1/1 in a perfectly ordered layer. The presence of lattice vacancies can explain the observed variability in the O/Ti ratio on the surface.

It was not possible to equate the observed 2D phases on the Pt_3Ti surface to any plane of the known bulk Ti oxide phases. This result is not unexpected. The structure of a single layer is affected by the interaction with the substrate and by the different bonding geometry, so that it should not necessarily correspond to the structure derived from the bulk lattice. Other oxides are known to form 2D phases which are unrelated to the bulk phases (11). In all of the 2D layer phases observed here, (except in the hexagonal one on the (100) face), at least one of the sides of the unit cell is 3.3 or 3.4 Å long. This distance does not correspond to the Ti-Ti distance in TiO (NaCl type lattice: 2.95 Å) nor to the Ti-O-Ti (linear) distance in the same oxide (4.18 Å). No obvious coincidence with the substrate forces the overlayer to assume this particular dimension. To explain this recurrence we can take into account the fact that in an undistorted TiO (111) layer, formed by one hexagonal layer of titanium and one of oxygen, the oxygen atoms sit in three-fold sites forming a bond angle of 90° with the titanium atoms. In the bulk solid this angle results from the octahedral coordination of oxygen atoms. However, in a 2D TiO (111) layer growing on the Pt_3Ti surface, octahedral holes do not exist. In such a case, the overlayer may relax its structure to form the "natural" tetrahedral oxygen bonding angle of 108.5 degrees, with an

oxygen atom at the center of the tetrahedron and titanium atoms at the vertices, as illustrated in Figure 8. The Ti-Ti distance must become equal to 3.4 Å in order to maintain the Ti-O distance equal to 2.09 Å as in bulk TiO. With a small distortion, the group of three Ti atoms forming the basis of the tetrahedron can form the basic unit of the distorted hexagonal structure of the $\begin{bmatrix} 1.20 & \overline{0.14} \\ 0 & 1.24 \end{bmatrix}$ phase. The 3.4 Å distance is formed also if we consider the oxygen atoms as sitting on "bridge" position on two titanium atoms. The 3.4 Å distance is also present in all of the single layer "TiO" phases observed on Pt_3Ti (100) (Table 2). In these phases, the effect of the substrate-overlayer bond on the dimension and the orientation of the unit cell, is even more evident. The most affected phase is the $\begin{bmatrix} 1 & \overline{0.57} \\ 0 & 1.14 \end{bmatrix}$ hexagonal phase. This phase contains less oxygen than the others and the smaller number of Ti-O bonds may cause the substrate-overlayer (probably Ti-Pt) bond to become more important in affecting the overlayer structure. Here the spacing between the compact {11} rows of the overlayer is equal to the interatomic distance in the substrate.

After the formation of the first layer of titanium oxide, the multilayer phase starts growing with two different mechanisms on the two types of single crystal faces. On the (111) face, the absence of double diffraction features indicates the immediate formation of multilayer clusters, while on the (100) face the initial presence of double diffraction spots indicates the formation of uniform epitaxial multilayers (two or three layers at most). This difference in behavior may be tentatively explained as due to a better match of the multilayer rectangular unit cell with respect to the square unit cell of the (100) substrate, which permits

the formation of some well-defined long range coincidences, as evidenced by the cell periodicity: $\begin{bmatrix} 3.0 & \overline{3.33} \\ 1 & 0.9 \end{bmatrix}$. On the hexagonal substrate surface, (111), coincidences would require a large distortion of the overlayer cell. However, as oxidation of either face proceeds, multilayer clusters eventually form, which should be closely related to one of the known bulk titanium oxides. After an exhaustive examination of the lattice parameters of all known titanium oxides (12), we found that the only acceptable agreement is obtained by the (031) plane of the "$TiO_{1.20}$" oxide described by Hilti in Reference 13. The data relative to this comparison are reported in Table 4. The agreement is not perfect but it may be considered reasonable, taking into account the imprecision in the LEED measurements and the possibility that the lattice parameters may vary when the phase is present as a very thin film. All of the other known titanium oxide phases give a considerably worse agreement. For instance, in Ti_3O_5 the (001) plane is centered-rectangular (as the phases observed by LEED), but the long side of the unit cell is equal to 9.452 Å (14), compared with the value of 12 - 12.4 Å obtained from the LEED observations. Such disagreement (about 30%) is too high to be acceptable. The "$TiO_{1.20}$" phase is derived from the TiO lattice (fcc, NaCl type) by removing part of the titanium atoms, thereby forming an ordered vacancy lattice. The (031) plane is a high density plane derived from the TiO (100) plane and is depicted in Fig. 13. Hilti (13) reports that the $TiO_{1.20}$ stoichiometry results from the fact that not all the lattice points defined as vacancies are empty (if such were the case of the stoichiometry would be $TiO_{1.50}$). It is therefore possible that the actual stoichiometry of this phase depends on the conditions of growth and it may therefore be slightly different than

"$TiO_{1.20}$." AES observations of the titanium peak shape indicate that the O/Ti ratio is higher than 1 and is therefore consistent with this interpretation of the LEED patterns, but we cannot derive the actual stoichiometry from this. We should also consider the possibility that the "holes" in the "$TiO_{1.20}$" lattice are filled with Pt atoms, in which case the stoichiometry of the overlayer would be "$PtTi_2O_3$." This interpretation does not contradict the experimental data, but it is not supported by any specific observation. Some mixed Pt/Ti/O compounds are reported in literature (15), but none with the stoichiometry "$PtTi_2O_3$."

The final step in the oxidation of Pt_3Ti, in extreme conditions ($T > 1000^{\circ}$ K, $Po_2 > 10^{-5}$ torr), is the formation of TiO_2, which is expected since TiO_2 is thermodynamically the most stable of the titanium oxides. The exposure to oxygen in these conditions causes complete phase separation of the alloy components even in the bulk of the crystal.

However, probably as a result of the strong Pt·Ti intermetallic bond, the nature of the phase separation during oxidation of Pt_3Ti is very different from that in some other intermetallic catalysts, such as $LaNi_5$ (16) and other rare earth- transition metal combinations (17). In Pt_3Ti, the oxide layer growth is uniformly "vertical," with relatively small gradients in Ti concentration parallel to the metal-oxide interface. In $LaNi_5$ and like compounds, the rare earth oxide separates "horizontally" so that metallic Ni and rare earth oxide coexist separately on the surface. These distinctions in surface structure would have a profound effect on the catalytic properties of the two types of surfaces: in Pt_3Ti, oxidation

causes growth of a compact oxide overlayer that blocks all the active (metallic) surface; in $LaNi_5$, oxidation causes growth of oxide clusters having open metallic surface available for catalysis.

CONCLUSION

The growth of a titanium oxide overlayer on the Pt_3Ti surface upon exposure to oxygen occurs in three stages, which are distinguished by differences in both the oxygen pressure and the surface temperature. The initial stage of oxidation is the segregation of Ti onto the surface to form a single layer (2D) oxide phase. The 2D layer has "TiO" stoichiometry and a structure where titanium atoms probably form a compact plane bonded to the substrate surface and oxygen atoms are situated on top of the titanium layer. The formation of this 2D phase occurs by the formation of patches on the surface which, upon completion of a monolayer, block all the metallic sites for chemisorption. The growth of the 2D phase results in the depletion of titanium from the underlying subsurface region. At a sufficiently high temperature and pressure, multilayer oxide growth can be initiated. The multilayer phase has been identified as "$TiO_{1.20}$", a phase derived from the TiO (NaCl type) lattice by removing a number of titanium atoms to form the ordered vacancy lattice. Oxidizing in extreme conditions (atmospheric pressure, 1273° K), causes complete phase separation and covers the surface with a thick film of TiO_2 (rutile), the thermodynamically favored oxide of titanium.

ACKNOWLEDGMENT

This work was supported by the Assistant Secretary for Fossil Energy, Office of Fuel Cells, Advanced Concepts Division under Contract No. DE-AC03-76SF00098 and by the Office of Naval Research, Department of Defense

under Contract No. N-00014-82-F-0055. The authors are indebted to Messrs. B. Addis and J. Holthuis for the preparation of the Pt_3Ti crystals, to Professor G. Rovida for advice and helpful discussion on the interpretation of the LEED data, and to Dr. D. Boone for his assistance in obtaining funding for this study.

Table 1 LEED Results, Pt Ti(111).

PHASE	SYMMETRY	a,b Å	ANGLE	NOTES
$Pt_3Ti(111)$	hexagonal	5.51, 5.51	120°	Clean Surface. Values of a and b taken from Ref. (5).
$\begin{bmatrix} 1.20 & \overline{0.14} \\ 0 & 1.24 \end{bmatrix}$	quasi-hexagonal	3.5, 3.4	125.5°	Monolayer phase. 2 domains rotated 11° with respect to each other. O(508 eV)/Ti(387 eV) ≃ 1.2;Ti(387 eV)/Pt(237 eV) = 2.8. Probable stoichiometry: TiO.
$\begin{bmatrix} 0.53 & \overline{1.96} \\ 1.43 & 1.43 \end{bmatrix}$	oblique	6.3,3.94	108°	Two equivalent unit cells for the same phase: primitive (oblique) or centered rectangular. Multilayer. O (508 eV)/Ti(387 eV) ≧ 1.5; Ti(387 eV)/Pt(237 eV) ≧ 12.7. Probable stoichiometry: $TiO_{1.20}$.
or	or	or	or	
$\begin{bmatrix} 2.5 & \overline{2.5} \\ 1.43 & 1.43 \end{bmatrix}$	centered rectangular	12.0, 3.94	90°	

Table 2. LEED Results, $Pt_3Ti(100)$.

PHASE	SUMMETRY	a,b Å	ANGLE	NOTES
$Pt_3Ti(100)$	square	3.898, 3.898	90°	Clean surface. a and b taken from Ref. (5).
$\begin{bmatrix} 1.5 & 0 \\ 0 & 1.2 \end{bmatrix}$	rectangular	4.1, 3.3	90°	Single layer phase. Forms at high O_2 pressure. O(508 eV)/ Ti(387 eV) ≃ 1.2. Probable stoichiometry: TiO. Several domains observed.
$\begin{bmatrix} 2 & \overline{0.3} \\ 0 & 1.2 \end{bmatrix}$	oblique	5.6, 3.3	98.5°	Single layer phase. Forms at intermediate O_2 pressure. O(508 eV)/Ti(387 eV) = 0.9-1.4. Probable stoichiometry: TiO. Several domains observed.
$\begin{bmatrix} 1 & \overline{0.57} \\ 0 & 1.14 \end{bmatrix}$	hexagonal	3.15, 3.15	120°	Single layer phase, forms at low oxygen pressure and high T. O(508 eV)/Ti(387 eV)≃ 0.7. Probable stoichiometry: TiO_x with $x < 1$. Several domains observed.

Table 2. (cont.)

PHASE	SYMMETRY	a,b Å	ANGLE	NOTES
$\begin{bmatrix} 1.0 & \overline{2.1} \\ 1.0 & 0.9 \end{bmatrix}$	oblique	6.4, 3.7	107°	Two equivalent unit cells for the same phase: primitive (oblique) or centered rectangular. Multilayer. O(508 eV)/Ti(387 eV) $\geq$ 1.5. Probable stoichiometry: $TiO_{1.20}$. Several equivalent domains observed.
or	or	or	or	
$\begin{bmatrix} 3.0 & \overline{3.33} \\ 1.0 & 0.9 \end{bmatrix}$	centered rectangular	12.4, 3.7	90°	

Table 3. Summary of the AES Analysis of Surface Composition after Oxidation of Pt_3Ti.

Oxidation Conditions	Phase Formed	Ti(387 eV)/Pt(237 eV) AES Ratio	O(508 eV)/Ti(387 eV) AES Ratio
No exposure	Clean Pt_3Ti	1.9 (polycryst)	0
$1x10^{-8}$ - $1x10^{-5}$ torr O_2 at 600-1000 K (or: atm pressure at room temperature)	"TiO" phases single layer	1.9-3.5	0.7-1.4
$1x10^{-6}$ - $5x10^{-5}$ torr O_2 at 800-1200 K	"$TiO_{1.20}$ phases multilayer	3.5-14	1.5-1.6
Atm pressure 1273 K	TiO_2 rutile multilayer phase	∞(Pt peaks not detectable)	2.8

Table 4. Comparison of LEED Data Relative to Multilayer Structures Observed on Pt_3Ti and Data Relative to the $TiO_{1.20}$ Bulk Phase (13).

	$TiO_{1.20}$ Bulk Phase (03$\bar{1}$) Plane	$\begin{bmatrix} 2.5 & \overline{2.5} \\ 1.43 & 1.43 \end{bmatrix}$ Structure on $Pt_3Ti(111)$	$\begin{bmatrix} 3.0 & \overline{3.33} \\ 1.0 & 0.9 \end{bmatrix}$ Structure on $Pt_3Ti(100)$
a(Å)	3.986	3.94	3.7
b(Å)	12.748	12.0	12.4
α	90°	90°	90°

REFERENCES

1. P.J. Meschter and W.L. Worrell, Met. Trans., 7A, 299 (1976).
2. L. Brewer, Viewpoint of Stability of Metallic Structures in "Phase Stability of Metals and Alloys," eds. P. Rudman and R.I. Jaffee. McGraw-Hill, NY, p. 39, 1967.
3. U. Bardi, G.A. Somorjai and P.N. Ross, J. Catal. 85, 272 (1984).
4. P.N. Ross, Electric Power Research Institute, Report EM-1553, September 1980.
5. U. Bardi and P.N. Ross, to be published in Surface Science.
6. F.P. Netzer and J.A.D. Matthew, J. Electron Spectr. and Related Phenomena, 16, 359 (1979).
7. C.R. Brundle, Surface Sci., 48, 99 (1975).
8. G.D. Davis, M. Natan and K.A. Anderson, Applications of Surface Science, 15, 321 (1983).
9. G. Derry and P.N. Ross, Surf. Sci., 140 (1984).
10. U. Bardi, P.N. Ross and G.A. Somorjai, J. Vac. Sci. Technol. A, 2, 40 (1984).
11. P.J. Goddard and R.M. Lambert, Surface Sci., 117, 519 (1981).
12. Landolt-Bornstain, Springer-Verlag Berlin, Heidelberg, NY, 1980, Vol. 7, pp. 289-310 and references therein.
13. E. Hilti, Z. Naturwissenschaften, 55, 130 (1980).
14. S. Asbrink and A. Magneli, Acta Chem. Scand., 11, 1606 (1957).
15. M.V. Nevitt, J.W. Downey and R.A. Morris, Trans. Met. Soc. AIME, 218, 1019 (1960).
16. H.C. Siegmann, L.W. Schlapbach and C.R. Brundle, Phys. Rev. Lett., 40, 972 (1978).
17. W.E. Wallace, "Rare Earth Intermetallics", Academic Press, New York, 1973

FIGURE CAPTIONS

1. (left) LEED patterns observed after oxygen dosing of $Pt_3Ti(111)$: a.) LEED pattern designated "quasi-hexagonal" observed at 68 eV for a O(508)/Ti(387 eV) AES ratio = 1.2; b.) LEED pattern designated "$TiO_{1.2}$" multilayer pattern superimposed on the "quasi-hexagonal" pattern observed at 78 eV for a O(508)/Ti(387 eV) AES ratio $\geq$ 1.5. (right) Reciprocal space structures derived from the corresponding LEED pattern on left: large circles = substrate spots; small filled circles = overlayer spots; small open circles = double diffraction spots.

2. (upper panel) LEED patterns observed after oxygen dosing of $Pt_3Ti(100)$: a.) "rectangular" pattern observed at 68 eV for O(508 eV)/Ti(387 eV) AES ratio = 1.2 superimposed on C(2x2) pattern from the $Pt_3Ti(100)$ substrate; b.) "oblique" pattern observed at 66 eV for O(508)eV)/Ti(387 eV) $\simeq$ 1.5; c.) "hexagonal" pattern observed at 84 eV for O(508 eV)/Ti(387 eV) AES ratio = 0.7 superimposed on the c(2x2) pattern from the substrate; d.) "$TiO_{1.2}$" pattern at 35 eV for O(508 eV)/Ti(387 eV) AES ratio $\geq$ 1.

(lower panel) Reciprocal space structures derived from corresponding LEED patterns: large filled circles = substrate spots, small filled circles = overlayer spots, small open circles = double diffraction spots.

3. Oxygen uptake curves for increasing exposures (pressure) on the three types of Pt_3Ti surfaces studies. All doses were for 30 sec at 773 K.
4. CO TDS peak intensity from partially oxidized Pt_3Ti surfaces as a function of the Ti(387 eV)/Pt(237 eV) AES ratio. The data indicate a complete blocking of the Pt adsorptive sites for an AES ratio higher than about 3.4.
5. AES spectra of the $Pt_3Ti(111)$ surface (2 keV, $2V_{pp}$): a.) "clean" surface after ion bombardment and annealing, Ti(387 eV)/Pt(237 eV) = 1.9; b.) surface obtained after exposure to oxygen at 800 K, Ti(387 eV)/Pt(237 eV) = 4.2; note the absence of the small peak at 395 eV indicating a "TiO" stoichiometry (8); the O(509)/Ti(387 eV) = 0.8 since the surface was annealed in vacuum after oxidation causing a partial reduction as described in the text; this surface gave the "quasi-hexagonal" LEED pattern; c.) surface obtained by exposure to oxygen at 800 K, $2x10^{-5}$ torr O_2. Ti(387 eV)/Pt(237 eV) ratio = 11.6; note the appearance of the peak at 395 eV and the increase of the relative intensity of the oxygen peak indicating a higher degree of oxidation; LEED pattern was that of Fig. 1b.
6. Effect of temperature on the amount of titanium oxide formed on the polycrystalline Pt_3Ti surface by exposure at constant oxygen pressure (30 sec at $5x10^{-6}$ torr).
7. Reduction of the titanium oxide overlayer segregated onto the Pt_3Ti polycrystalline surface by annealing (60 sec) in hydrogen ($2x10^{-6}$ torr). The overlayer surface was obtained by oxygen dosing the clean annealed Pt_3Ti surface 30 sec at $5x10^{-6}$ torr O_2, 773 K.

8. Schematic model for the 2D "TiO" structure consistent with the recurrent dimension of 3.4 Å (the Ti-Ti distance) and the Ti-O bond distance of 2.1 Å as in cubic TiO.

9. Schematic model of the $TiO_{1.20}$ multilayer phase segregating onto the $Pt_3Ti(100)$ surface. A similar structure applies for the $Pt_3Ti(111)$ surface as well. Large circles indicate oxygen atoms, small circles indicate titanium atoms. The rectangular centered overlayer cell is outlined. Oxygen atoms occupying octahedral positions on top of Ti atoms in the plane depicted are not shown. Note the presence of lattice vacancies in the oxide layer. The arrow designated a_o is the scale dimension of the lattice constant (the Ti-Ti distance) for Pt_3Ti.

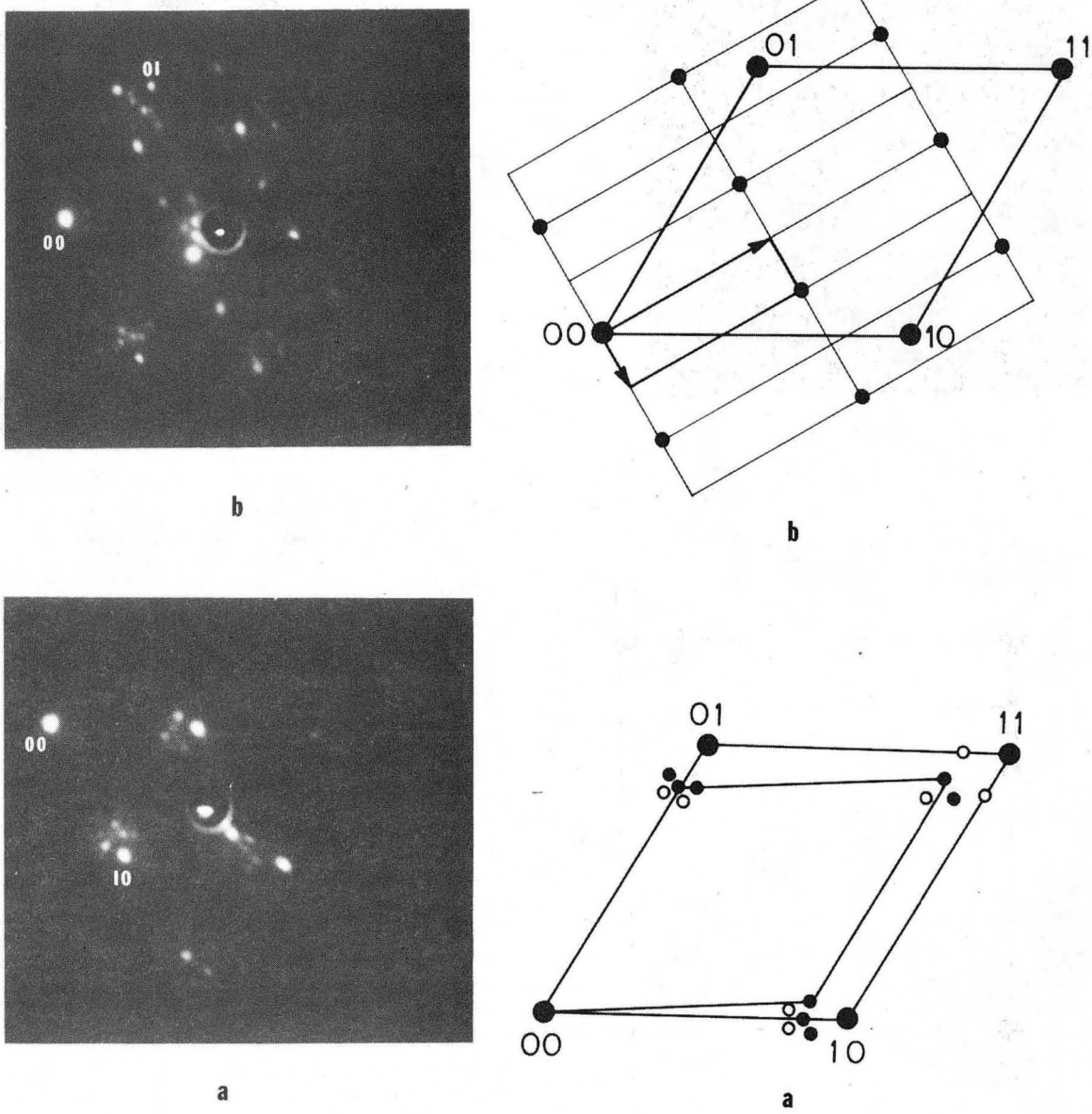

XBB843-2270

Fig. 1

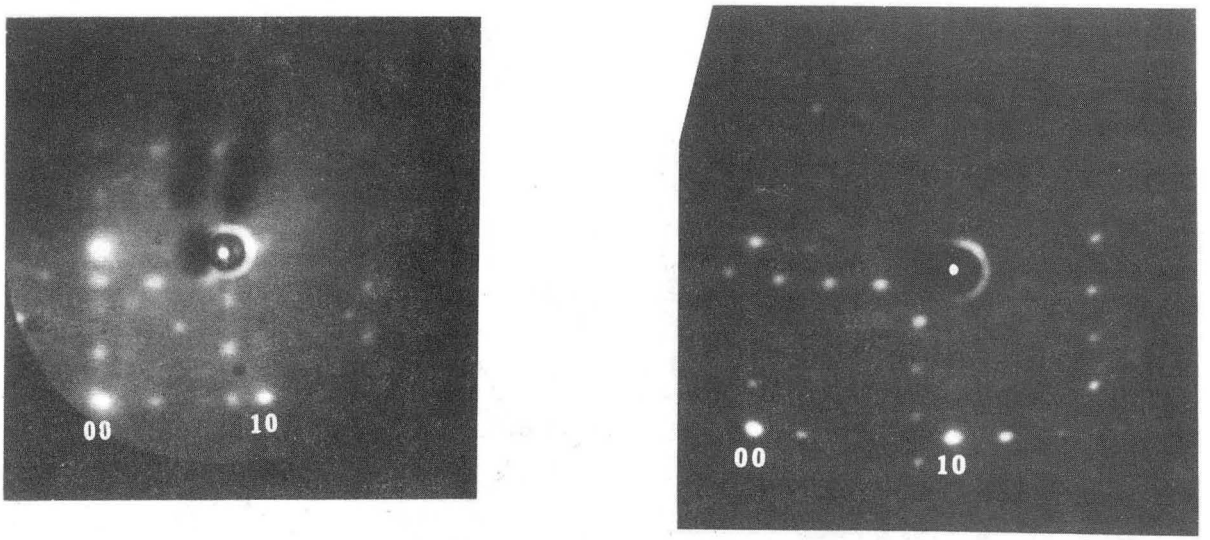

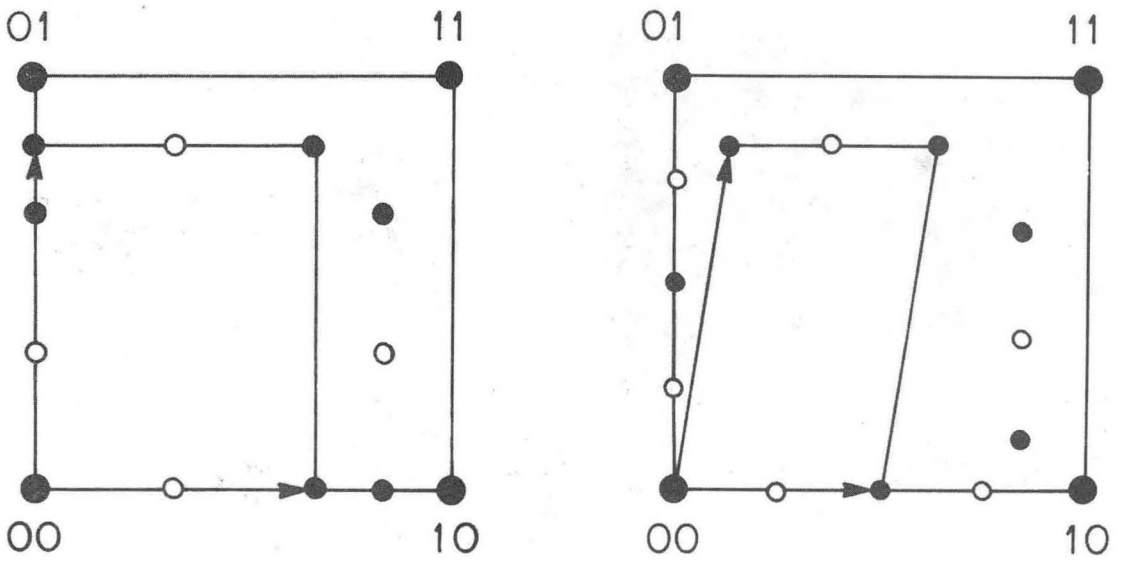

a b

XBB843-2269

Fig. 2. (upper panel)

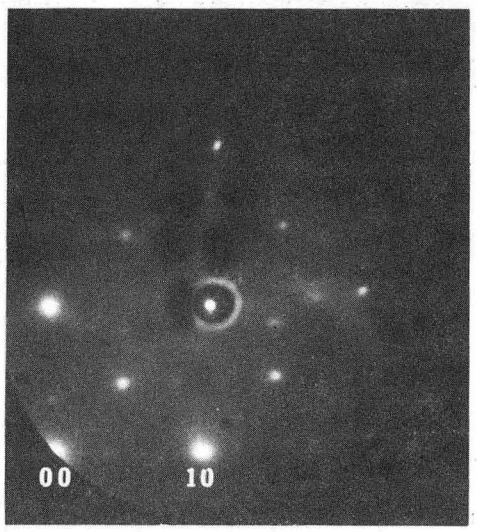

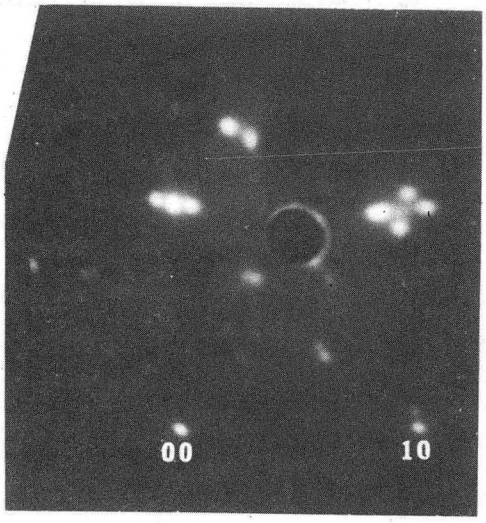

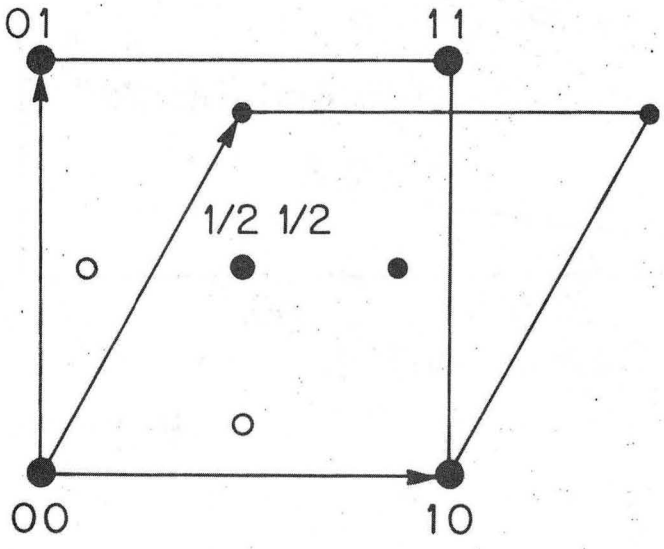

c

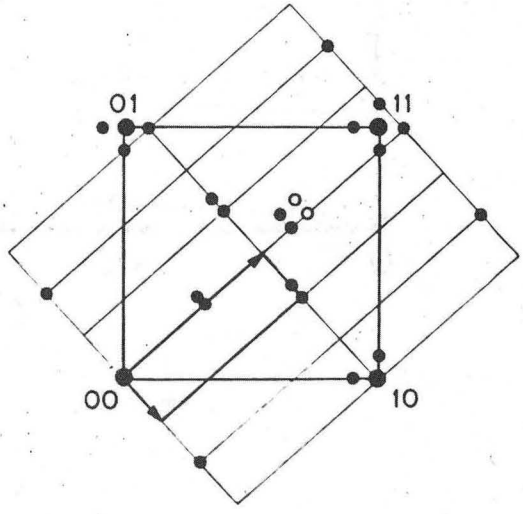

d

XBB843-2268

Fig. 2. (lower panel)

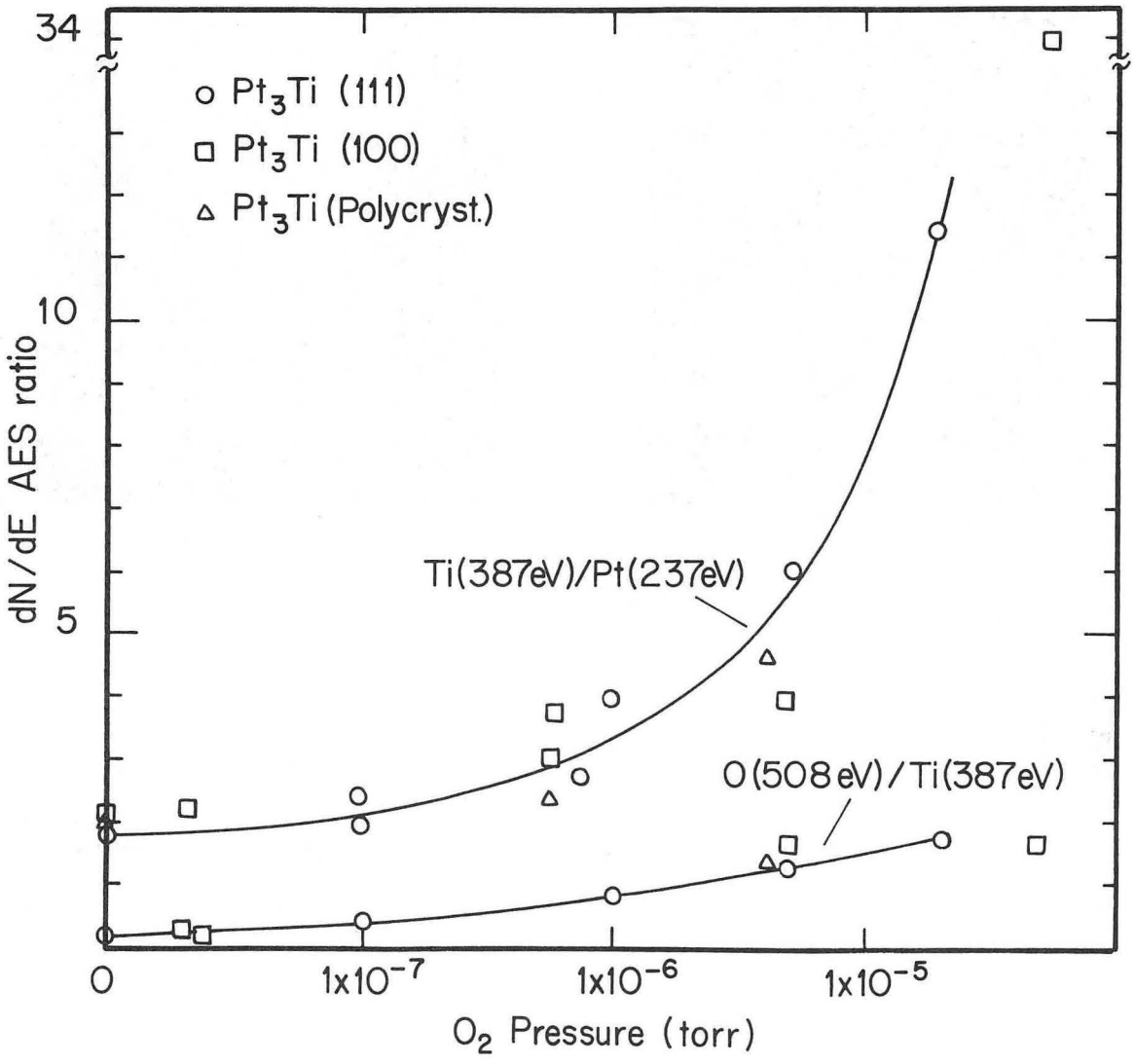

XBL 843-1229

Fig. 3

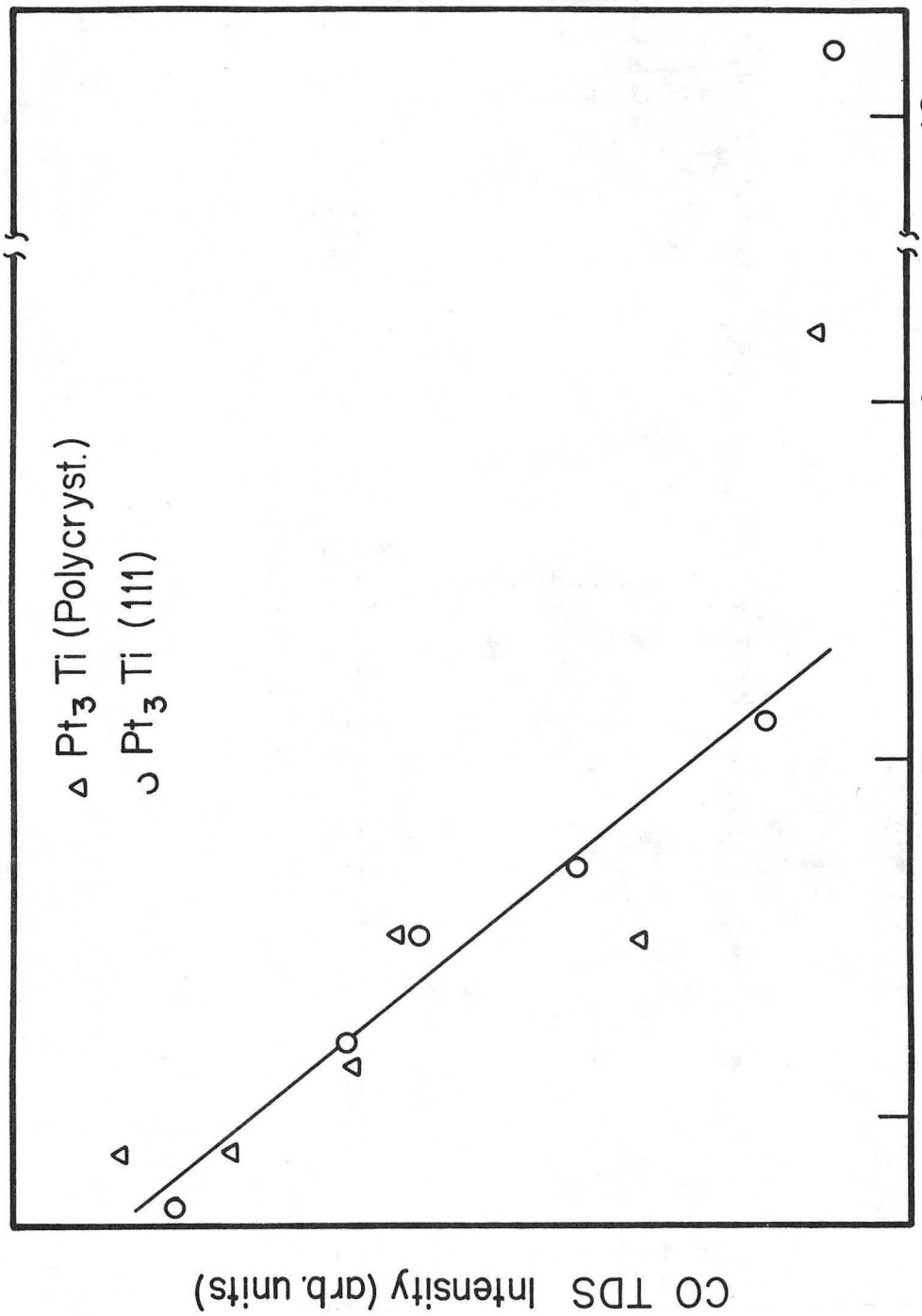

XBL 843-1166

Fig. 4

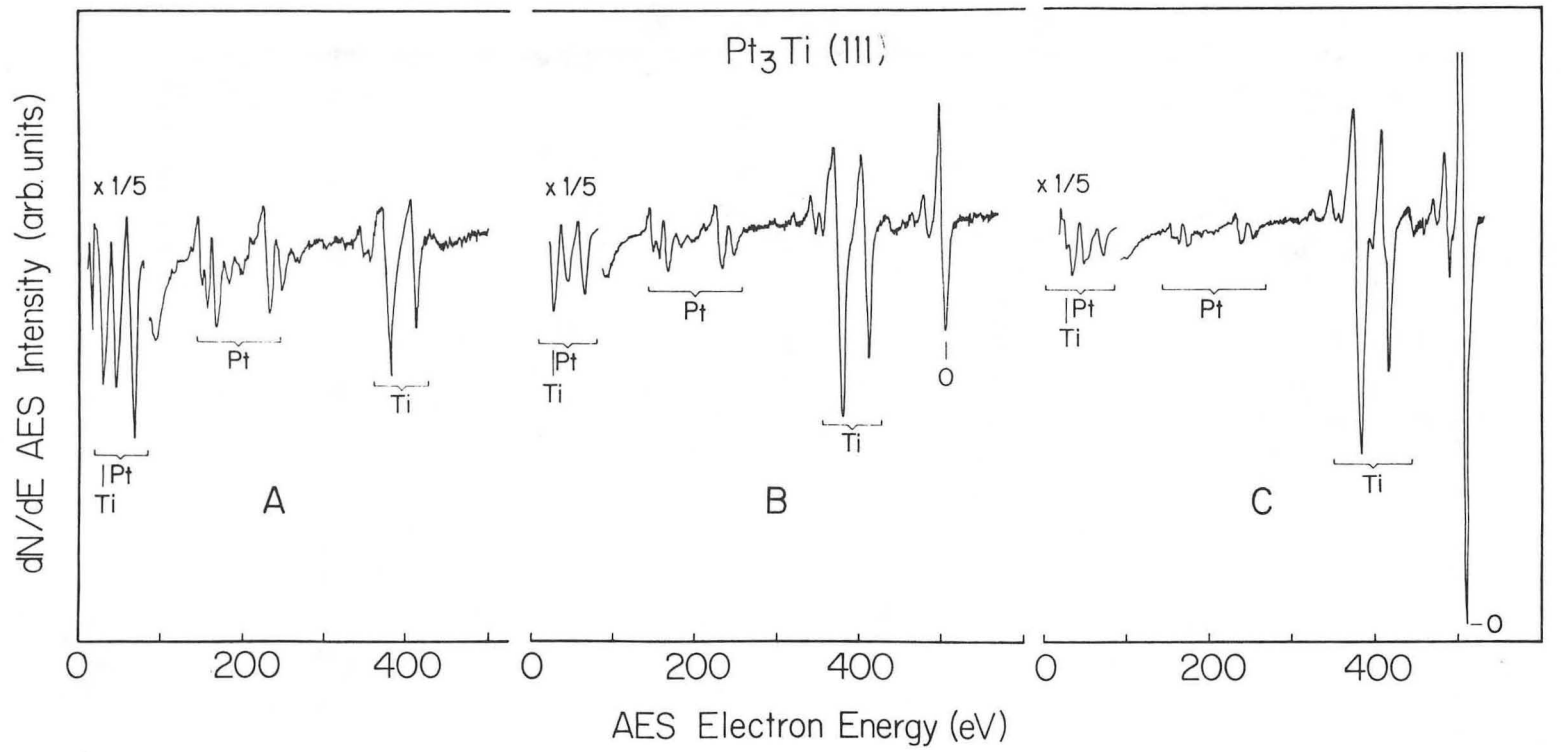

XBL 843-1168

Fig. 5.

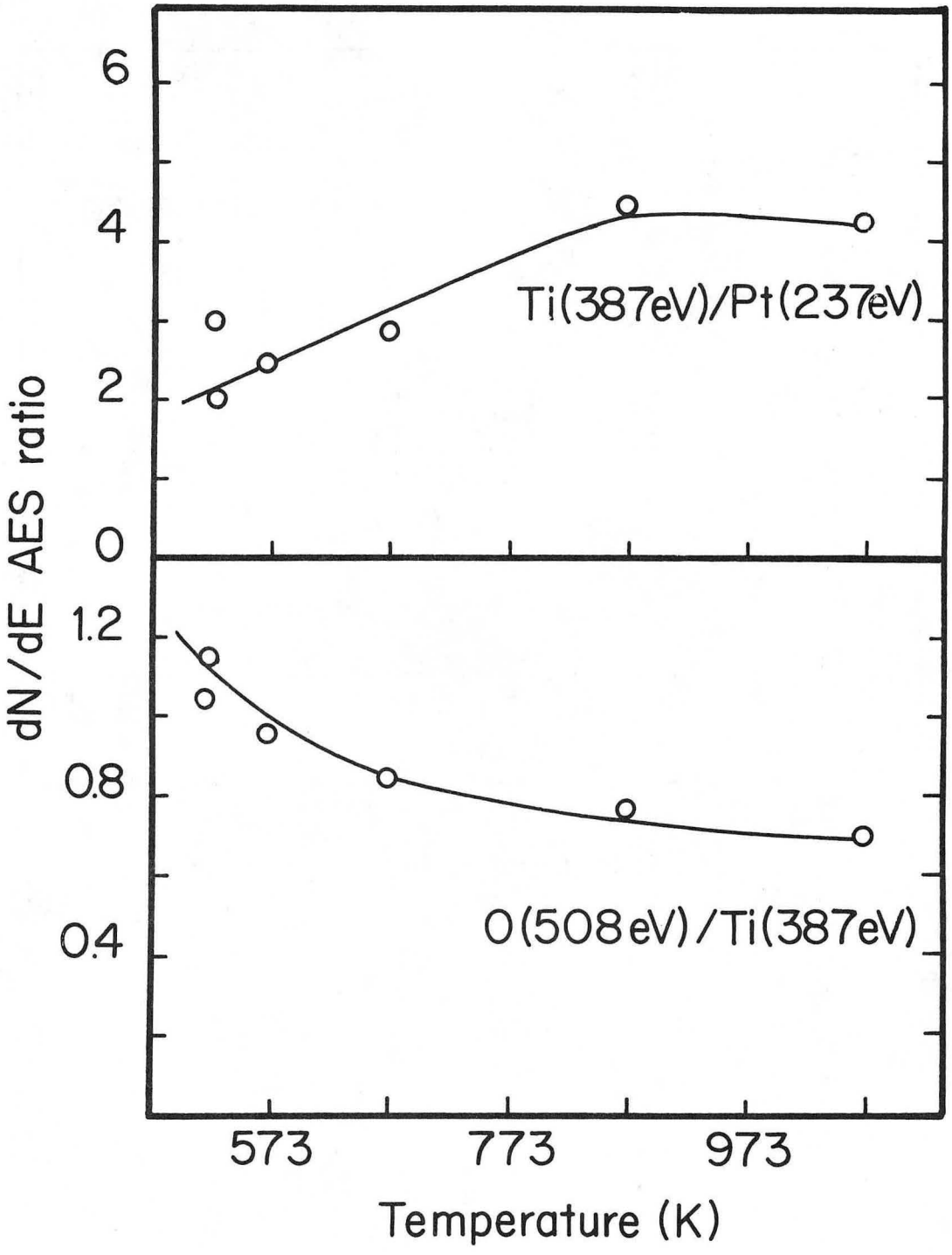

XBL 843-1165

Fig. 6

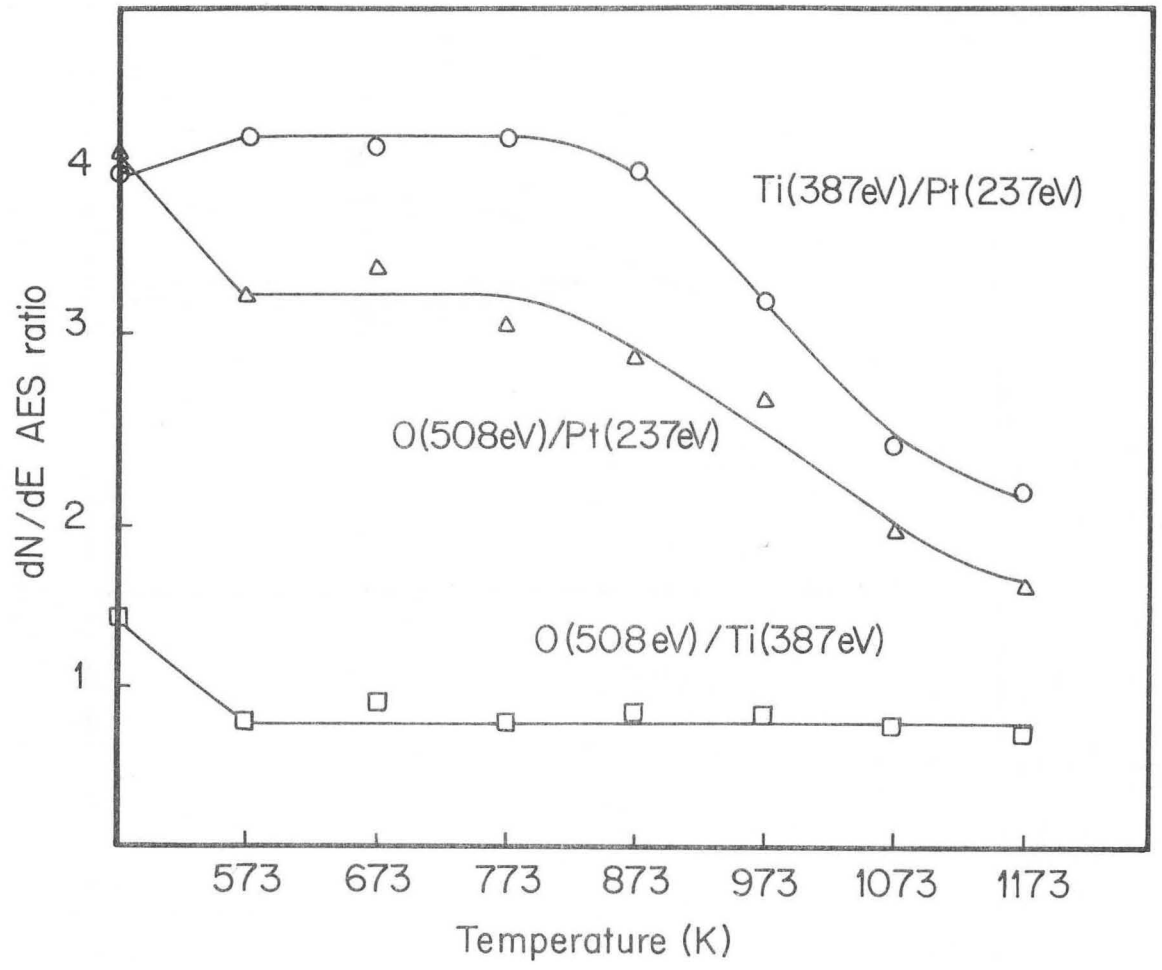

XBL 843-1230

Fig. 7

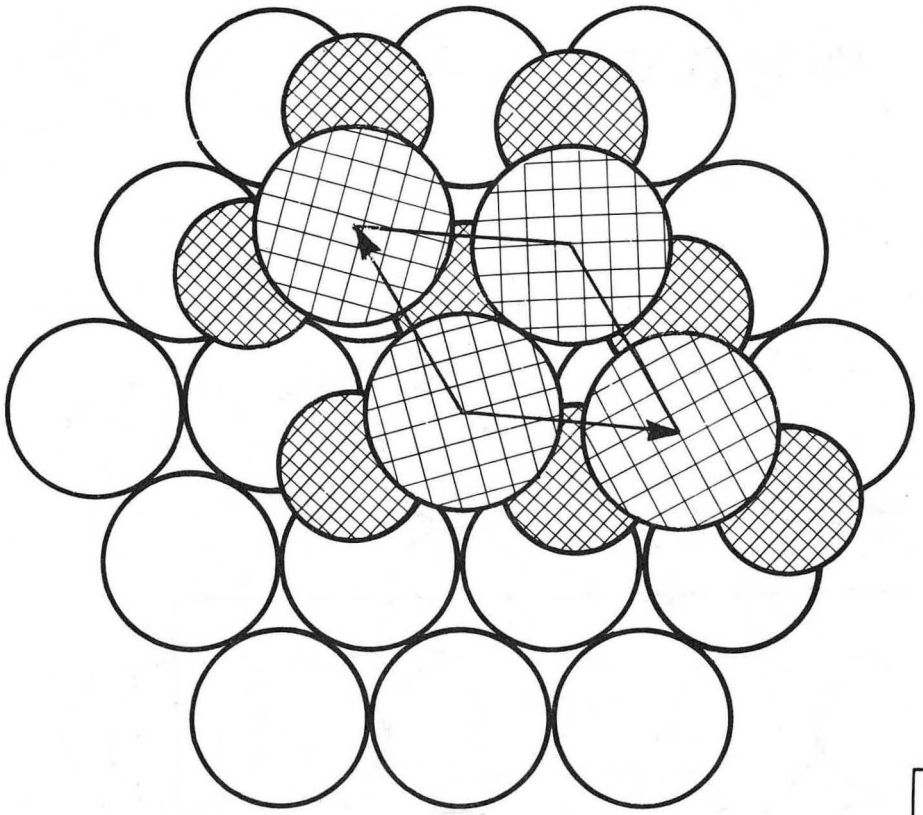

$$\begin{bmatrix} 1.20 & \overline{0.14} \\ 0 & 1.24 \end{bmatrix}$$

XBL 844-10503

Fig. 8

Pt_3 Ti (100) – "Ti $O_{1.20}$"

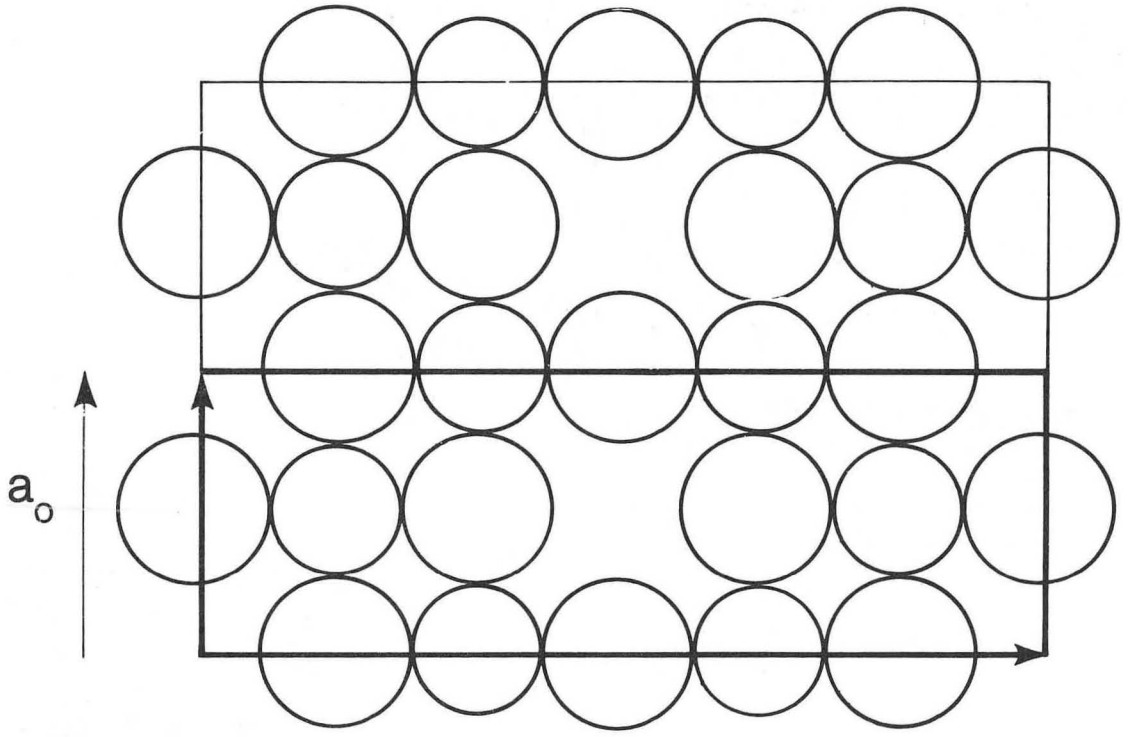

XBL 844-10502

Fig. 9

TECHNICAL INFORMATION DEPARTMENT
LAWRENCE BERKELEY LABORATORY
UNIVERSITY OF CALIFORNIA
BERKELEY, CALIFORNIA 94720